ALMA Observations of Supernova Remnant N49 in the Large Magellanic Cloud. II. Non-LTE Analysis of Shock-heated Molecular Clouds

Poster # S6.4

Hidetoshi Sano[1] ([1]Gifu University, sano.hidetoshi.w4@f.gifu-u.ac.jp) Sano et al. (2023) ApJ, 958, 53

Co-Authors: Y. Yamane[2], J. Th. van Loon[3], K. Furuya[4], Y. Fukui[2], R. Z. E. Alsaberi[5], A. Bamba[6], R. Enokiya[4], M. D. Filipovic[5], R. Indebetouw[7], T. Inoue[8], A. Kawamura[4], M. Lakicevic[9], C. J Law[7], N. Mizuno[4], T. Murase[1], T. Onishi[10], S. Park[11], P. P. Plucinsky[12], J. Rho[13], A. M. S. Richards[14], G. Rowell[15], M. Sasaki[16], J. Seok[17], P. Sharda[18], L. Staveley-Smith[19], H. Suzuki[8], T. Temim[19], K. Tokuda[8], K. Tsuge[6], K. Tachihara[2]

([2]Nagoya U., [3]Keele U., [4]NAOJ, [5]WSU, [6]U. of Tokyo, [7]U. of Virginia, [8]Konan U., [9]AOB, [10]Osaka Metropolitan U., [11]U. of Texas, [12]CfA, [13]SETI, [14]U. of Manchester, [15]U. of Adelaide, [16]FAU, [17]U. of Missouri, [18]Leiden U., [19]Princeton U.)

Personal H.P. Paper Access

ABSTRACT We present the first compelling evidence of shock-heated molecular clouds associated with the supernova remnant (SNR) N49 in the Large Magellanic Cloud (LMC). Using ^{12}CO(J = 2–1, 3–2) and ^{13}CO(J = 2–1) line emission data taken with the Atacama Large Millimeter/Submillimeter Array, we derived the H_2 number density and kinetic temperature of eight ^{13}CO-detected clouds using the large velocity gradient approximation at a resolution of 3.5 arcsec (~0.8 pc at the LMC distance). The physical properties of the clouds are divided into two categories: three of them near the shock front show the highest temperatures of ~50 K with densities of ~500–700 cm^{-3}, while other clouds slightly distant from the SNR have moderate temperatures of 20 K with densities of ~800–1300 cm^{-3}. The former clouds were heated by supernova shocks, but the latter were dominantly affected by the cosmic-ray heating. These findings are consistent with the efficient production of X-ray recombining plasma in N49 due to thermal conduction between the cold clouds and hot plasma. We also find that the gas pressure is roughly constant except for the three shock-engulfed clouds inside or on the SNR shell, suggesting that almost no clouds have evaporated within the short SNR age of ~4800 yr. This result is compatible with the shock-interaction model with dense and clumpy clouds inside a low-density wind bubble.

1. Magellanic supernova remnant N49

- Core-collapse / Mixed morphology
  (e.g., Gaensler et al. 2001; Klose et al. 2004; Badenes et al. 2009; Yamaguchi et al. 2014)
- Diameter：~18 pc (or ~1.3 arcmin)
  (e.g., Dickel et al. 1993; Warren et al. 2003; Bozzetto et al. 2017)
- Age：~4800 yr
  (Park et al. 2012)
- Bright in optical, IR, UV, and X-rays
  (e.g., Dickel & Milne 1998; Park et al. 2003, 2012; Sankrit et al. 2004; Bilikova et al. 2007; Otsuka et al. 2010)
- Soft gamma-ray repeater 0526–66
  (e.g., Gaensler et al. 2001; Park et al. 2012)
- Recombining Plasma
  (Uchida et al. 2015)
- GMC is associated with the SE shell
  (Banas et al. 1997; Yamane, Sano et al. 2018)

2. ALMA CO observations

Project Number (PI)..... 2015.1.01195.S (**J. Th. van Loon**) + 2019.1.01400.S (**H. Sano**)
Target line..................... ^{12}CO(J = 1–0, 2–1, 3–2), ^{13}CO(J = 2–1) (Band 3+6+7)
Observed area............. ~1' × 1' (Band 3: single pointing, Band 6+7: mosaic mode)
Antennas...................... 12-m × 45–46, 7-m × 10–11, TP × 3 (ACA stand alone for Band 7)
Beam size..................... **~3.19" × 2.25" for ^{12}CO(J = 1–0), ~1.73" × 1.10" for ^{12}CO(J = 2–1)**
~1.82" × 1.14" for ^{13}CO(J = 2–1), ~3.48" × 2.76" for ^{12}CO(J = 3–2)
RMS noise level........... ~0.07 K (Band 3), ~0.09 K (Band 6), and ~0.11 K (Band 7) at 0.4 km s^{-1}

3. Spatial Distributions of CO and X-rays

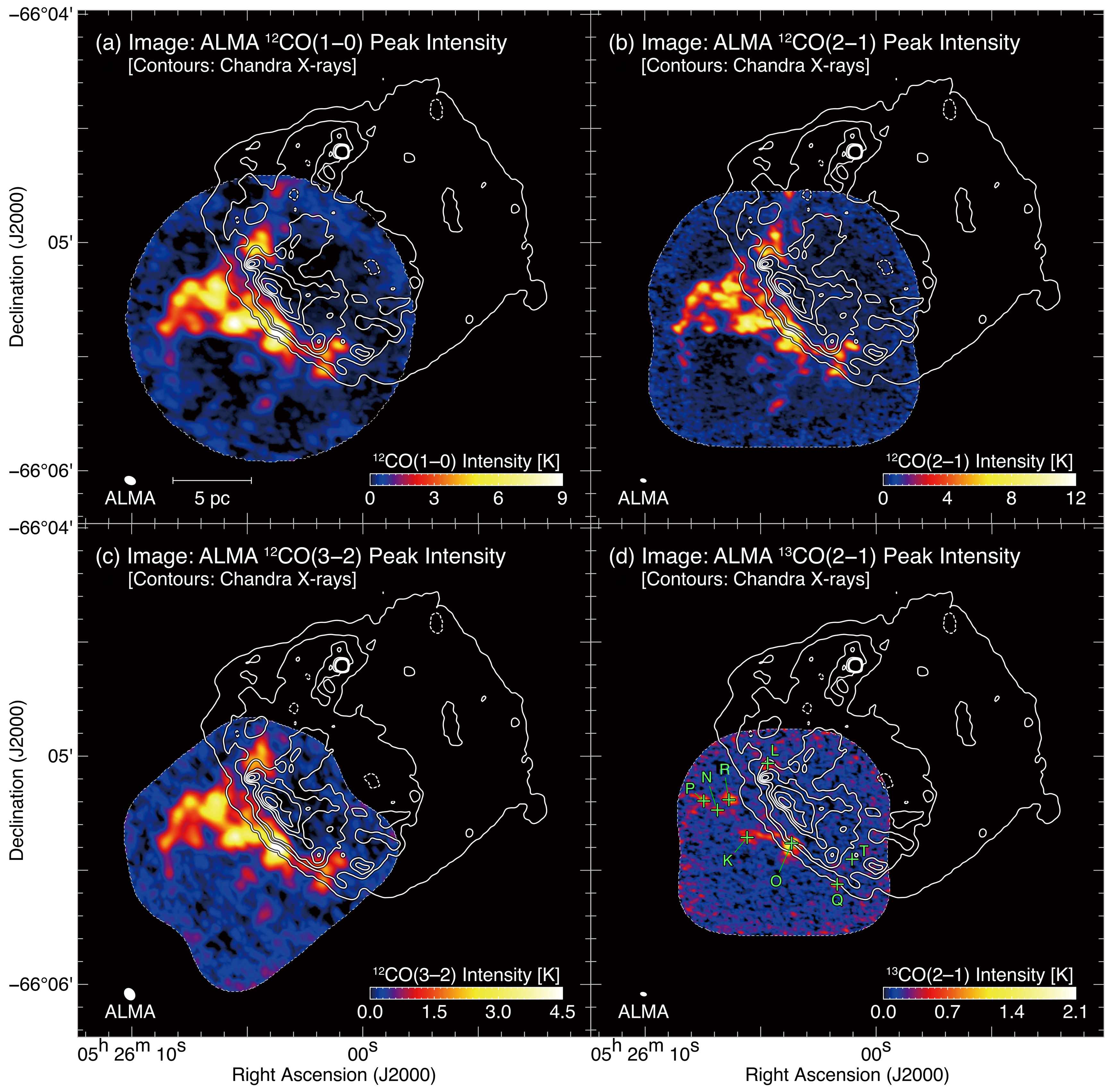

Figure 1. Peak intensity maps of (a) ^{12}CO(J = 1–0), (b) ^{12}CO(J = 2–1), (c) ^{12}CO(J = 3–2), and (d) ^{13}CO(J = 2–1). The velocity range of CO is from 285.5 to 287.8 km s^{-1}. Superposed contours represent Chandra X-ray intensity in the energy band of 0.5–7.0 keV. The lowest contour level and the contour intervals are 5 × 10^{-7} and 3 × 10^{-6} photons pixel^{-1} s^{-1}, respectively. The regions enclosed by dashed lines indicate the observed areas using ALMA. The CO peaks K, L, N, O–R, and T defined by Yamane et al. (2018) are also indicated in (d).

4. Physical Properties of CO Clouds

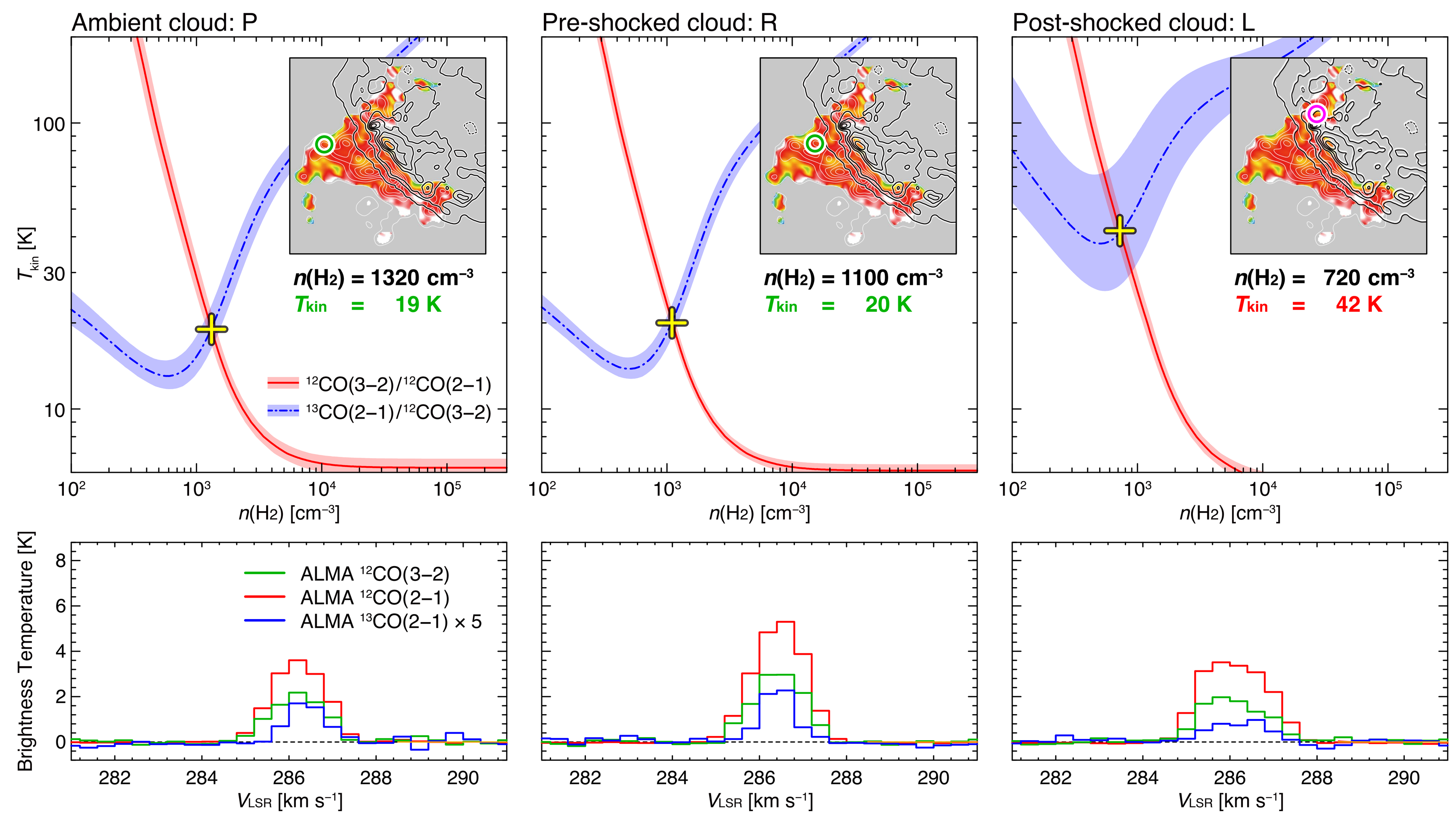

Figure 2. Top panels: large velocity gradient results on the number density of molecular hydrogen, $n(H_2)$, and the kinetic temperature, T_{kin}, for the ambient cloud P, pre-shocked cloud R, and the post-shocked cloud L. The red lines and blue dashed-dotted lines indicate the intensity ratios of ^{12}CO(J = 3–2)/^{12}CO(J =2–1) and ^{13}CO(J = 2–1)/^{12}CO(J =3–2), respectively. The shaded areas surrounding the red and blue lines indicate the 1σ ranges of each intensity ratio. Yellow crosses represent the best-fit values of $n(H_2)$ and T_{kin} for each cloud. The spatial positions and best-fit values for each cloud are shown in the top-right corners for each panel. Bottom panels: CO intensity profiles for clouds P, R, and L. The physical properties of each cloud are summarized in Table 1.

Name	α_{J2000}	δ_{J2000}	T_b			V_{peak}	ΔV	Size	M_{vir}	R_{dist}	T_{kin}	$n(H_2)$
			^{12}CO(3–2)	^{12}CO(2–1)	^{13}CO(2–1)							
	(h m s)	(° ′ ″)	(K)	(K)	(K)	(km s^{-1})	(km s^{-1})	(pc)	($M_\odot$)	(pc)	(K)	(10^3 cm^{-3})
(1)	(2)	(3)	(4)	(5)	(6)	(7)	(8)	(9)	(10)	(11)	(12)	(13)
K	5:26:5.5	−66:05:21	3.60	6.59	0.35	285.5	0.83	1.3	80	10.7	45^{+14}_{-9}	$0.53^{+0.05}_{-0.06}$
L	5:26:4.7	−66:05:02	2.00	3.75	0.18	286.3	1.72	1.2	340	7.7	42^{+26}_{-13}	$0.72^{+0.13}_{-0.14}$
N	5:26:6.7	−66:05:15	2.58	4.67	0.40	286.4	0.40	0.8	10	11.6	21^{+4}_{-3}	$0.78^{+0.02}_{-0.04}$
O	5:26:3.7	−66:05:23	4.91	8.26	0.91	286.2	0.69	1.2	50	8.8	19^{+1}_{-2}	$1.10^{+0.01}_{-0.01}$
P	5:26:7.5	−66:05:12	2.17	3.70	0.36	286.4	1.00	1.1	100	12.2	19^{+4}_{-3}	$1.32^{+0.01}_{-0.03}$
Q	5:26:1.7	−66:05:34	1.82	3.64	0.25	286.5	0.90	1.0	80	9.6	21^{+6}_{-4}	$0.81^{+0.06}_{-0.05}$
R	5:26:6.3	−66:05:11	3.17	5.49	0.51	286.4	0.86	1.1	80	10.7	20^{+3}_{-2}	$1.10^{+0.02}_{-0.03}$
T	5:26:1.0	−66:05:27	1.55	2.94	0.14	286.4	0.57	0.9	30	7.7	46^{+57}_{-18}	$0.48^{+0.09}_{-0.14}$

Table 1. (1): Cloud name defined by Paper I. (2, 3): Position of the maximum intensity of ^{12}CO(J = 1–0) (Yamane et al. 2018). (4–8): Physicalproperties of CO emission derived from a single Gaussian fitting. All the CO data sets were smoothed to match the beam size of 3.5" × 3.5". (4–6): Peak brightness temperature of ^{12}CO(J = 3–2), ^{12}CO(J = 2–1), and ^{13}CO(J = 2–1) emision. (7): Central velocity of ^{13}CO(J = 2–1) spectra. (8): FWHM line width of ^{13}CO(J = 2–1) spectra. (9): ^{13}CO(J = 2–1) derived cloud size defined as $(A/\pi)^{0.5} \times 2$, where A is thetotal cloud surface area surrounded by the half intensity of peak integrated intensity contour. (10): Mass of the cloud derived using the virial theorem and ^{13}CO(J = 2–1) properties. (11): Radial distance from the geometric center of the SNR at (α_{J2000}, δ_{J2000}) = (5^{h}25^{m}59.57^s, 66°04'56.4"). (12): Kinetic temperature. (12): Number density of molecular hydrogen.

5. Discussion and Summary

Shock heating and partial evaporation of the clouds

The negative correlation between T_{kin} and $n(H_2)$ as shown in Figure 3a indicates that clouds N, O, P, Q, and R have constant pressure and did not experience shock evaporation within the short SNR age of ~ 4800 yr. On the other hand, clouds K, L, and T, which are on the inside or on the edge of the shell, are significantly shifted from this pressure-constant line to a higher-pressure region and have slightly reduced densities, suggesting that the shock-engulfed clouds were partially evaporated through the shock–cloud interaction. The decreased density and increased pressure (and kinetic temperature) of the shocked molecular clouds have important implications for understanding the negative feedback of energetic supernova shocks on star formation. Also, our discovery of shock-heated clouds is consistent with the thermal conduction origin of the recombining plasma between the cold/dense clouds and plasma (Uchida et al. 2015).

Cosmic-ray heating of the pre-shock clouds

Considering the time evolution of T_{kin} as a function of cosmic-ray ionization rates ζ using a PDR model (Figure 3b, see also Furuya et al. 2022), we found that the pre-shock clouds are exposed to ~200 times more cosmic rays than the solar value. Therefore, the observed values of T_{kin} ~20 K at pre-shock and ambient clouds can be explained as the cosmic ray heating effect.

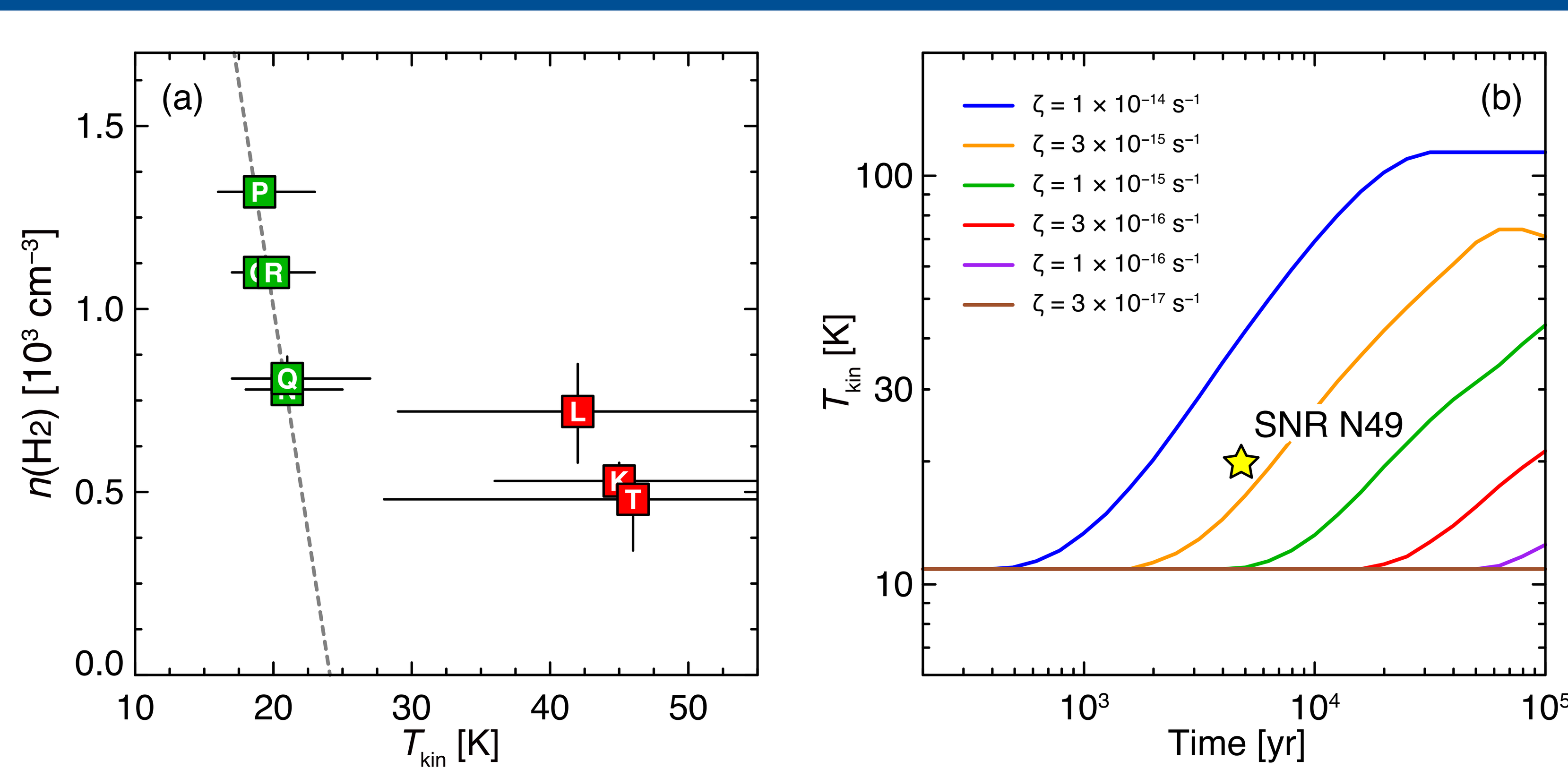

Figure 3. (a) Scatter plot between T_{kin} and $n(H_2)$. The dashed line indicates the linear regression using the least-squares method except for the CO clouds L, K, and T. (b) Time evolution of kinematic temperature T_{kin} at the cloud center after the supernova event that generates SNR N49. Colors indicate the assumed cosmic-ray ionization rate ζ from 3 × 10^{-17} s^{-1} to 1 × 10^{-14} s^{-1}. The star symbol indicates the observed values of Tkin for the ambient or pre-shocked clouds at the age of N49 (4800 yr).